considerably shorter than the thermal charging. The reason for this is that for the major portion of the discharging process during which the temperature of the PCM downstream of the LHSPB remains at the melting/freezing point, there is a constant temperature difference between the vapor inlet and vapor exit temperatures. This difference is larger than the corresponding difference in the charging process, i.e., the difference between the vapor inlet temperature and the melting point of the PCM during the charging process is only 19 K, whereas during the discharging process the difference between the vapor inlet temperature and the freezing point of the PCM is 31 K. Hence, energy is stored at a lower rate in the charging process than energy is removed during the discharging process for the portions of these processes under discussion. Again, this fact can easily be seen from Fig. 3 in which the difference between the rate of heat flow into and out of the packed bed is shown.

Conclusions

The transient processes of thermal charging and discharging of a SHSPB and a LHSPB with a compressible working fluid were simulated. The investigations showed distinctly different energy storage characteristics for these two kinds of packed beds. The high-energy storage density of the LHSPB was clearly observed from the studies carried out. For the two energy storage materials considered, although the density of the sensible heat storage material (1% Carbon-steel) was approximately nine times larger than that of the PCM (myristic acid), the total energy storage capacity of the LHSPB was higher.

Use of a compressible working fluid and accounting for the inertia effects in the vapor phase momentum equation resulted in a time-dependent mass flow rate through the packed bed.

Also, in the case of the LHSPB it was observed that the thermal charging and discharging times differed considerably. The main reason for this difference is that for a major portion of the charging or discharging process the PCM temperature downstream of the packed bed remains constant at the melting/freezing temperature of the PCM. An important conclusion which was obtained from our results is that the closer the PCM melting/freezing temperature is to the charging temperature (vapor inlet temperature during thermal charging mode) the longer will be the time taken for charging and the shorter will be the time taken for discharging of the packed bed. Likewise, the closer the PCM melting/freezing temperature is to the discharging temperature (vapor inlet temperature during thermal discharging mode) the longer will be the time taken for discharging and the shorter will be the time taken for charging of the packed bed.

Acknowledgments

The support by Aero Propulsion Laboratory of the U.S. Air Force under Contract F33615-89-C-2949 and the grant by OSC for this investigation is acknowledged and appreciated. The authors would also like to acknowledge J. E. Beam, W. Chang and T. Mahefkey for their support and help in this work.

References

[1]Riaz, M., "Analytical Solutions for Single- and Two-Phase Models of Packed Bed Thermal Storage Systems," *Journal of Heat Transfer*, Vol. 99, August 1977, pp. 489–492.

[2]Beasley, D. E., and Clark J. A., "Transient Response of a Packed Bed for Thermal Energy Storage," *International Journal of Heat and Mass Transfer*, Vol. 27, No. 9, 1984, pp. 1659–1669.

[3]Gross, R. J., Hickox, C. E., and Hackett, C. E., "Numerical Simulation of Dual-Media Thermal Energy Storage Systems," *Journal of Solar Energy Engineering*, Vol. 102, 1980, pp. 287–293.

[4]Pitts, D. R., and Hong, J.S., "Analysis of the Transient Thermal Performance of a Latent Heat Storage Packed Bed," *Multiphase Transport in Porous Media* ASME FED-Vol. 60, HTD-Vol. 91, 1987, pp. 51–54.

[5]Ananthanarayanan, V., Sahai, Y., Mobley, C. E., and Rapp, R. A., "Modeling of Fixed Bed Heat Storage Units Utilizing Phase Change Materials," *Metallurgical Transactions B*, Vol. 18B, June 1987, pp. 339–346.

[6]Vafai, K., and Sozen, M., "Analysis of Energy and Momentum Transport for a Flow of a Gas through a Porous Bed," *Journal of Heat Transfer*, Vol. 112, August 1990, pp. 660–669.

Convective Heat Transfer Across a Duct with Asymmetric Blowing

H. J. Deacon Jr.* and D. A. Wallace†
The Aerospace Corporation,
El Segundo, California 90009

Introduction

A THERMAL protection system for advanced reusable hypersonic vehicles uses the evaporation of ice in a wicking material to protect the substructure from excessive heating. In the concept, refractory metal tiles supported by low-conductance thermal standoffs are subjected to the aerodynamic forces and heating of re-entry. The wick, which lies between the tiles and substructure, is heated by radiation from the tiles and convection through steam released from upstream evaporation. The steam convection problem may be modeled as the flow between an impermeable upper wall and a porous lower wall with fluid injection. No previous solutions to this problem were found. In an initial attempt to model the flow and heat transfer, similarity solutions of the incompressible, constant property Navier-Stokes and energy equations were sought. Preliminary design analysis suggested that the Reynolds number based on the mass blowing rate of the steam and the Peclet number would be of order unity. Therefore, a wide range of solutions were sought at higher and lower values of these parameters. The basic approach of White et al.[1] and Berman[2] was adopted to obtain solutions to the Navier-Stokes equations. Similarity solutions to the energy equation are found for the boundary layer approximation with viscous dissipation neglected for constant wall temperatures. The present problem is different from the work of Refs. 1 and 2 because only one wall is porous in this work and because solutions to the energy equation are also obtained. These solutions are used to obtain heat transfer rates to the upper and lower walls. The computed results can then be used for improved design analysis of the thermal protection system.

Solution of Navier-Stokes Equations

In this work, the flow is assumed to be two dimensional, incompressible, steady, and laminar with negligible body forces. The evaporation of the ice is simulated by a porous lower plate having a constant and uniform normal velocity.

The mass and momentum conservation equations are simplified to

$$\frac{\partial u}{\partial x} + \frac{1}{h}\frac{\partial v}{\partial \lambda} = 0$$

$$u\frac{\partial u}{\partial x} + \frac{v}{h}\frac{\partial u}{\partial \lambda} = -\frac{1}{\rho}\frac{\partial p}{\partial x} + \nu\left(\frac{\partial^2 u}{\partial x^2} + \frac{1}{h^2}\frac{\partial^2 u}{\partial \lambda^2}\right) \tag{1}$$

$$u\frac{\partial v}{\partial x} + \frac{v}{h}\frac{\partial v}{\partial \lambda} = -\frac{1}{\rho h}\frac{\partial p}{\partial \lambda} + \nu\left(\frac{\partial^2 v}{\partial x^2} + \frac{1}{h^2}\frac{\partial^2 v}{\partial \lambda^2}\right) \tag{2}$$

Received March 2, 1990; revision received Sept. 16, 1990; accepted for publication Sept. 26, 1990. Copyright © 1991 by the American Institute of Aeronautics and Astronautics, Inc. All rights reserved.

*Engineering Specialist, P.O. Box 92957, Los Angeles, CA 90009. Member AIAA.

†Member of the Technical Staff.

where λ is the normalized channel height (y/h) and the usual notation (see Ref. 1) has been adopted. The stream function

$$\psi = g(x)f(\lambda) \tag{3}$$

is adopted where the velocities are given by

$$u = \frac{\partial \psi}{\partial y} = \frac{1}{h}\frac{\partial \psi}{\partial \lambda} = \frac{1}{h} g f' \tag{4}$$

$$v = -\frac{\partial \psi}{\partial x} = -g' f \tag{5}$$

At the lower wall, $v = v_w$

$$v|_{\lambda=0} = -g'(x)f(0) = v_w$$

For a constant blowing velocity v_w, $g'(x)$ must also be a constant. This implies that $g(x)$ must be linear. No flow in the x direction is allowed at x equals zero. Therefore, it can be assumed that

$$g(x) = v_w x \tag{6}$$

where the zero point of x is the point of zero mass flow in the x direction (where the injected fluid splits into identical flows in opposite directions). After some manipulations the following expression is obtained:

$$\partial^2 P/\partial x \partial \lambda = 0 \tag{7}$$

Equation (1) then reduces to the following nonlinear ordinary differential equation where $Re = \rho v_w h/\mu$

$$Re(f'f'' - ff''') - f'''' = 0 \tag{8}$$

The boundary conditions for this fourth-order equation are obtained from setting the velocities of the upper and lower walls at appropriate values yielding

$$f(0) = -1 \quad f'(0) = 0 \quad f(1) = 0 \quad f'(1) = 0 \tag{9}$$

The nonlinear ordinary differential Eq. (8) subjected to the corresponding boundary conditions of f, as given by Eq. (9), was solved numerically using the Runge Kutta technique with a shooting method employed to satisfy the boundary conditions at the upper wall.

Once the velocity profiles are known, the pressure gradient along the channel can be extracted from Eq. (1). It can be written in the nondimensional form by dividing $\rho v_w^2/2h$

$$\left(\frac{\partial P}{\partial x}\right)^* = \frac{2}{Re}\cdot\frac{x}{h}f''' - 2\cdot\frac{x}{h}f'f' + 2\cdot\frac{x}{h}ff''$$

Solution of Energy Equation

Temperature profiles can be obtained from the solution of the boundary-layer approximation of the energy equation which is valid for long, low channels far from the initial point

$$\rho c_p\left(u\frac{\partial T}{\partial x} + \frac{v}{h}\frac{\partial T}{\partial \lambda}\right) = \frac{k}{h^2}\left(\frac{\partial^2 T}{\partial \lambda^2}\right) \tag{10}$$

where viscous dissipation has been neglected (valid for small values of the Eckert number). The separation of variables technique is applied to the energy equation. The temperature profiles are assumed to be

$$T(x, \lambda) = A(x)B(\lambda) \tag{11}$$

Following some algebraic manipulation

$$\left(\frac{x}{h}\right)\frac{A'(x)}{A(x)} = \frac{1}{f'}\left[\frac{\alpha}{h^2 v_w}\frac{B''(\lambda)}{B(\lambda)} + \frac{f}{h}\frac{B'(\lambda)}{B(\lambda)}\right] = k \tag{12}$$

where k must be a constant and α is the thermal diffusivity $k\rho c_p$. For this problem, the temperature T is normalized and maintained at fixed temperatures 0 and 1 at $y = 0$ and $y = h$, respectively, for all x. For example

$$T(x,0) = A(x)B(0) = 0$$

$$T(x,1) = A(x)B(1) = 1$$

Since $B(0)$ and $B(1)$ remain constant for all x, $A(x)$ must also remain constant for all x and from Eq. (12), k must be zero. Therefore, the temperature profiles are similar in the flow direction. Equation (12) is reduced to the following expression,

$$B''(\lambda) + Pe \cdot f \cdot B'(\lambda) = 0 \tag{15}$$

where Pe = Peclet number = $Re \cdot Pr$, Pr = Prandtl number, $B(0) = 0$, $B(1) = 1$.

Results and Conclusions

Dimensionless velocity profiles (f') were found numerically for various Reynolds numbers (1., 5., 10., and 20.) and are shown in Fig. 1. As expected, the profiles are not symmetrical with the centerline of the channel. As the Reynolds number increased, the profiles become more asymmetric. The pressure gradients are only slightly dependent on λ and the results are represented by the equation

$$\left(\frac{dP}{dx}\right)^* = (-0.028/Re - 0.006)\,x/h$$

Figure 2 presents the numerical results of the temperature profiles for a Reynolds number of 1 and Peclet numbers of 1., 5., 10., 20., and 50.

Results for dimensionless heat transfer (Nusselt number = $qhk_f/\Delta T$) at the upper and lower walls are presented in Fig. 3. The results are strongly affected by the Peclet number and moderately influenced by the Reynolds number. For Peclet numbers less than unity, solutions are dominated by conduction in the fluid and high-heat transfer rates exist at the blown wall. Higher Peclet numbers result in a significant decrease in heat transfer at the lower wall. Heat transfer at the upper wall increases with increasing Peclet numbers as expected due to the increased velocity gradient of the upper wall. It also shows a modest influence of Reynolds numbers.

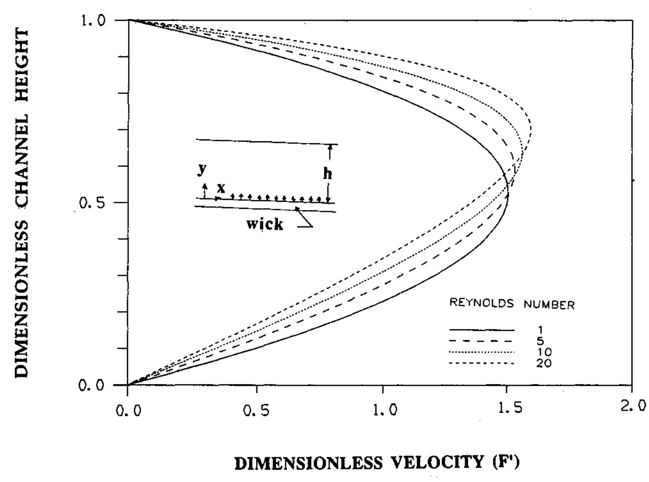

Fig. 1 Velocity profiles.

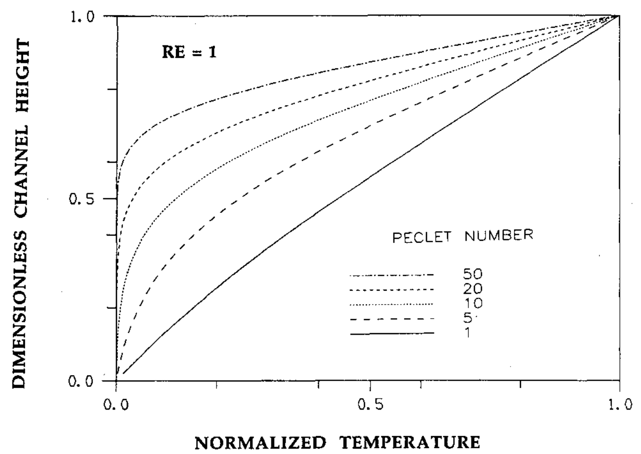

Fig. 2 Temperature profiles.

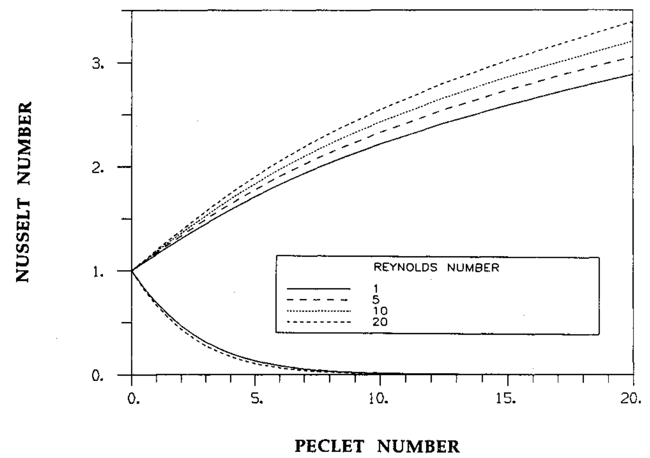

Fig. 3 Heat transfer rates at upper and lower walls.

The work presented here reveals several interesting conclusions about flow and heat transfer in a channel with injection at one wall. At low-blowing Reynolds numbers, the streamwise velocity profiles resemble Poiseuille flow. As the blowing increases, the profiles become more skewed with reduced velocity gradients at the injected wall. The pressure gradients along the channel decrease almost linearly with length, which reflects the increased pressure drop required to accelerate the injected fluid to the continually increasing velocities required by mass conservation.

The constant property assumption used in this work allows the momentum and mass conservation equations to be solved independently of the energy equation. Similarity solutions to the boundary-layer approximation of the energy equation with viscous dissipation neglected were found for several values of the Reynolds and Peclet numbers. The effects of Reynolds number on these solutions are not strong. However, very significant effects of the Peclet numbers are found. At Peclet numbers much less than unity ordinary conduction effects dominate and the temperature profile was found to be linear across the channel. As blowing increases, the profiles become increasingly nonlinear, with the temperature gradients (heat transfer rates) at the blown wall becoming smaller. This behavior is similar to that of a boundary layer on a transpiration cooled wall. For Peclet numbers greater than 3, the conduction to the blown wall is small. The opposite behavior occurs at the impermeable wall where heat transfer rates continually increase with increased blowing. These results can be used to approximate the transfer processes in thermal protection systems using a wick containing an evaporation material. The results show that high-evaporation rates can reduce heating of the substructure. Further, the increased convection at the upper wall can also be effective at reducing radiative heat transfer to the wick.

References

[1]White, Jr., F. M., Barfield, B. F., and Goglia, M. J., "Laminar Flow in a Uniformly Porous Channel," *Journal of Applied Mechanics*, Vol. 25, No. 4, 1958, pp. 613–617.

[2]Berman, A. S., "Laminar Flow in Channels with Porous Walls," *Journal of Applied Physics*, Vol. 24, No. 9, 1953, pp. 1232–1235.

Experimental Study of Natural Convection in Horizontal Porous Layers with Multiple Heat Sources

F. C. Lai* and F. A. Kulacki†
Colorado State University,
Fort Collins, Colorado 80523

Nomenclature

c = specific heat of fluid at constant pressure, J/kg-K
Da = Darcy number, K/H^2
d = diameter of glass bead, m
g = acceleration of gravity, m/s^2
H = height of the porous layer, m
h = average heat transfer coefficient on the heated surface, W/m^2-K
K = permeability of the saturated porous medium, m^2
k = effective thermal conductivity of the porous medium, W/m-K
Nu = average Nusselt number, hH/k
q = uniform heat flux, W/m^2
Ra = Rayleigh number, $Kg\beta qH^2/\nu\alpha k$
T = temperature, K
α = thermal diffusivity of porous medium, $k/(\rho c)_f$, m^2/s
β = isobaric thermal expansion coefficient of fluid, K^{-1}
θ = dimensionless temperature
ν = kinematic viscosity of fluid, m^2/s
ρ = density of fluid, kg/m^3
ϕ = porosity

Subscripts

f = fluid phase
s = solid phase

I. Introduction

OVER the past four decades, natural convection in saturated porous media has received considerable attention for its important applications in engineering and geophysics problems. However, most of the previous studies have considered the case of a horizontal porous layer uniformly heated from below, and emphases have been placed on the establishment of the criteria for onset of convection. Very few results have been reported for the case of a discrete heat source, although problems of this type are encountered more fre-

Presented as Paper 90-0257 at the AIAA 28th Aerospace Sciences Meeting, Reno, NV, Jan. 8–11, 1990; received Dec. 12, 1989; accepted for publication May 4, 1990. Copyright © 1989 by the American Institute of Aeronautics and Astronautics, Inc. All rights reserved.

*Research Associate, Department of Mechanical Engineering. Member AIAA.

†Dean, College of Engineering, 111 Engineering Building.